Al-Khwarizmi Engineering Journal
Al-Khwarizmi Engineering Journal
ISSN (printed): 1818 – 1171, ISSN (online): 2312 – 0789
Vol. 21, No. 3, September, (2025), pp. 106- 117

Pulse Wave Speed Estimation: A Comparative Study of the PU-Loop Technique versus Tensile and Compliance Testing on Synthetic Elastic Tubes

Wisam S. Hacham[1*], Falah Alzuwaid[2], and Wesam Al-Zubaedi[3]
[1] *Mechatronics Engineering Department, Al-Khwarizmi College of Engineering, University of Baghdad, Baghdad, Iraq*
[2] *Trafford and Stockport College Group (TSCG), Stretford, Construction & Sustainability, Manchester, United Kingdom*
[3] *Wigan and Leigh College, United Kingdom*
*Corresponding Author's Email: wisam@kecbu.uobaghdad.edu.iq

(Received 16 June 2025; Revised 26 July 2025; Accepted 3 August 2025; Published 1 September 2025)
https://doi.org/10.22153/kej.2025.08.003

Abstract

Pulse wave speed (*c*) is a key variable in haemodynamics and cardiovascular system analysis. It is directly related to arterial elasticity and inversely to distensibility of the arterial lumen. The pressure–velocity loop (PU-loop), derived from simultaneous velocity (*U*) and pressure (*P*) measurements, is used to estimate *c*, leveraging the linear *U*–*P* relationship during early systole, when reflected waves are absent due to bifurcations and/or occlusion. The PU-loop method was validated using tensile and compliance testing. Tensile testing, using a load cell, estimated Young's modulus (*E*) of synthetic elastic tubes, allowing *c* calculation using the Moens–Korteweg equation. Compliance testing under static pressure assessed the relation between *P* and volume (*V*). This relationship predicted the compression and contraction courses, validating the testing applied to the lumen of the particular flexible tube. Consequently—to calculate the distensibility of the flexible tube lumen—the change in internal lumen volume due to the change in *P* was used, hence *c* corresponding to the Bramwell–Hill equation. Despite limitations such as sample size of tested specimens, experimental conditions not fully physiological, sensitivity of testing due to measurement noise; neglecting anisotropicity and heterogeneity of vessels; not accounting for the full complexity of real arterial behaviour and the use of synthetic elastic tubes stiffer than in vivo lumens, the calculated *c* ($c_{calculated}$), using the PU-loop technique, was in agreement with values acquired from compliance- and tensile-testing-based calculations. According to compliance and tension testing, the velocity of *c* was 19.5±0.05 and 19.5±0.012.1 m/s, respectively. Using the PU-loop technique, it was 20±0.25 m/s. These results validate the PU-loop methodology in *c* assessment.

Keywords: *Bramwell–Hill equation; Compliance testing; Moens–Korteweg equation; PU-loop; Tensile testing*.

1. Introduction

Pulse wave velocity (*c*) has emerged as a critical clinical biomarker for assessing arterial stiffness, a robust predictor of cardiovascular morbidity. As the velocity at which pressure waves propagate through the arterial tree, *c* reflects the elastic properties of the vascular wall and is directly influenced by structural and functional changes in the arteries. Elevated *c* values are strongly associated with increased arterial stiffness and have been independently linked to a heightened risk of cardiovascular events, including hypertension, stroke and heart failure. Due to its non-invasive nature and predictive value, *c* is increasingly used in clinical practice and research settings to evaluate vascular aging, monitor disease progression and guide therapeutic interventions. Therefore, accurate and reproducible estimation of *c* is highly essential for early detection and risk stratification in cardiovascular practice. Moreover, precise determination of *c* is crucial for optimising the separation of variables in wave intensity analysis, a widely used methodology in haemodynamic studies. The reliability of this technique depends on the accurate calculation of *c*, which characterises the traveling wave within the arterial lumen. Methods for determining *c* typically fall into two categories: estimation based on arterial geometry, dimensions and elastic properties, and transit time measurements between two locations. Each approach has its own advantages and limitations. Transit time-based methods offer non-invasive average values of *c* across the measurement sites. By contrast, geometry-based methods require invasive measurements, which are difficult clinically.

c is a widely recognised clinical measure of arterial stiffness and plays a crucial role in assessing cardiovascular risk and vascular health [1, 2, 3]. Numerous methodologies have been developed to quantify local_*c* (c_{local}) and regional_*c* (c_{regional}), including sequential ultrasound-based measurements of diameter and velocity [4], forward-traveling pulse wave analysis [5] and pressure–volume loop (PU-loop) techniques [6]. The PU-loop method has been extensively investigated, revealing that wave reflections can lead to underestimation or overestimation of *c*, necessitating refined analytical corrections [7, 8]. Modelling and simulation studies enhanced our understanding of arterial haemodynamics, with simplified 1D models capturing complex wave interactions within the arterial network [9, 10]. Additional studies have demonstrated the influence of blood pressure on *c*, underscoring the importance of accounting for haemodynamic variability during clinical assessments [11, 12]. Recent recommendations emphasise the importance of standardises validation for non-invasive measurement devices [13] and highlight that (*c*) can effectively guide clinical decisions in cardiovascular disease management [14]. Comparative analyses have highlighted differences in measurement techniques [15, 16], and large-scale studies have confirmed *c*’s clinical relevance across diverse populations [17, 18]. Collectively, this body of evidence forms a robust foundation for the present study’s focus on refining *c* measurement techniques and their application in cardiovascular risk stratification.

c is a widely used biomarker of arterial stiffness and cardiovascular risk. Various methodologies were developed to measure it in vivo and in silico. Recent studies have underscored the importance of c_{local} measurements within the arterial tree for assessing regional differences in arterial stiffness [19], whereas techniques, such as pulse wave imaging, provide non-invasive and quantitative assessment of arterial stiffness in real time [20]. Elevated *c* has been shown to correlate with cognitive decline in elderly patients, highlighting its potential as a clinical tool for broader health assessments [21]. In addition, it has been utilised as a clinical measure to aid material characterization of vascular tissues [22], emphasising its role in diagnostic and research contexts. Real-time measurements of aortic *c* during exercise stress testing further expand its utility in dynamic physiological conditions [23]. Computational modelling frameworks, such as those developed by Bogatu et al. [24], have also contributed significantly to understanding *c* and arterial stiffness by simulating complex haemodynamic interactions. The distinction between central and peripheral arterial stiffness has been recognised as a critical factor in cardiovascular assessment, with early studies by Woodman et al. [25] illustrating the importance of site-specific measurements. The comparative studies of methodologies—including the landmark work by Salvi et al. [26]—have highlighted the need for standardisation and validation of *c* measurement techniques to ensure reliability and clinical applicability.

Finally, Janjua et al. [6] introduced a novel non-invasive method for estimating c_{local} using pressure–volume loop analysis. Pressure–volume loops were developed by simultaneously measuring pressure and flow waveforms at the same arterial site, thereby deriving c_{local} values. The researcher applied this technique to palmar digital arteries, showcasing its feasibility and potential for assessing arterial stiffness in peripheral vessels. The method offers a promising approach for non-invasively evaluating vascular health, particularly in settings where $c_{\mathrm{traditional}}$ measurement techniques may be challenging to implement.

In the arterial system, following the transmission of the initial compression wave and preceding the arrival of the backward pulse wave, which originates from discontinuities at reflection sites and returns to the measurement location, a period during cardiac systole exists when only forward waves are present. This time interval can be identified by examining the slope of the linear portion of the *U*–*P* loop during early cardiac systole [27].

The problem statement of this comparative study is to validate the application of the PU-loop technique for estimating *c*, with accuracy comparable to conventional mechanical testing approaches (e.g., tensile and compliance testing) under the static pressure conditions, when applied to synthetic elastic tubes. This validation required the estimation of the elastic properties of the synthetic flexible lumen. The Moens–Korteweg [28] and Bramwell–Hill [27] equations were applied to calculate pulse wave speed using compliance and tensile testing. The Moens–Korteweg equation requires knowledge of Young's modulus of elasticity, which was determined using a load cell (Instron High, Wycombe, UK). The Bramwell–Hill equation requires specification of the lumen's distensibility, which was obtained by performing a compliance test on the wall of the selected elastic rubber tube.

2. Methodology

The theoretical basis for calculating *c* is grounded in classical wave propagation theory, with the Moens–Korteweg and Bramwell–Hill equations representing the most widely accepted analytical models. These equations establish the relationship between *c* and the mechanical properties of the vessel wall and the enclosed fluid, subject to specific assumptions. The magnitude of *c* is quantified using the PU-loop technique, described in the following section. To validate this technique, Bramwell–Hill and Moens–Korteweg equations are used to determine *c*.

Methodological differences may lead to variations in the estimated values of *c*. Dynamic techniques (e.g., PU-Loop) assess *c* during the active phase of the cardiac cycle, reflecting real-time haemodynamic behaviour. By contrast, static approaches (e.g., tensile/compliance testing) derive *c* from passive vessel mechanics.

2.1 Wave Speed Determination

Khir et al. [29] originally presented the PU-loop technique. This method relies on the linearity between U and P of the pulse wave at the time interval where no backward reflected waves are present (e.g., early systolic upstroke where reflection effects are minimal). Accordingly, *c* can be written as follows:

$$c = \pm\,(dP/\rho dU)_{\text{LINEAR PORTION}} \qquad \ldots(1)$$

In equation 1, *dP* and *dU* represent the derivatives of *P* and *U* for any two consecutive sampling of the time interval during the early systole, respectively, and (ρ) indicates the fluid density. The time lag between *P* and *U* was accounted for prior to the analysis and was found to be ~6 ms. The time lag is caused by the dissimilarity of the frequency response of the measurement system.

The Moens–Korteweg equation results from elastic wave propagation theory for thin-walled cylindrical vessels. This formula is based on the following assumptions about the tube: it must be thin-walled, linearly elastic, incompressible and of uniform cylindrical shape. It is particularly well-suited to synthetic rubber tubes, which are apt to satisfy these assumptions in planned laboratory tests. The physical interpretability and general simplicity of this formula render it an excellent model for benchmarking mechanical behaviour in isotropic, homogeneous materials. This equation enables the calculation of *c* using the mechanical dimensions and properties of the tube lumen, expressed as follows:

$$c = (E.h/\rho.D)^{1/2} \qquad \ldots(2)$$

where *D*, *E* and *h* represent the uniform inner diameter, Young's modulus of elasticity and the tube wall thickness, respectively.

Bramwell–Hill equation: This equation is a relation between *c* and changes in vessel volume and pressure, but it is addressed to the fluid–vessel system compressibility and is best applied with pressure–volume data. It is also derived under the assumptions of axisymmetry and incompressibility of the vessel, which are reasonably well satisfied in experiments conducted on elastic–plastic tubes. This equation permits estimating *c* provided that the static pressure difference (dP) during compression and retraction strokes, as well as the volume change (dV) from the initial volume (V_o) are available. This equation can be written as follows:

$$c = (dP.V_0/\rho.dV)^{1/2} \qquad \ldots(3)$$

The application of the two traditional equations to synthetic rubber models is justified by their material uniformity, incompressibility and geometric simplicity, fitting closely the theoretical approximations of both models. Consequently, they provide a solid foundation for evaluating experimental methods and calibrating measurement systems prior to their application to more complex and biologically realistic geometries, an observation that holds true in our test setup.

2.2 Experimental setups

2.2.1 Long Tube Setup

The experimental setup used to estimate *c* utilising the PU-loop technique is shown in Fig. 1 [30]. All elements of the experiment are arranged on the same horizontal platform. The schematic illustrates the following key components: 1. reciprocating pump that mimics the cardiac function; 2. location of the haemostat valve; 3. catheter for pressure measurement at the designated site; 4. control unit of the pressure transducer [catheter]; 5. flow probe positioned 25 cm downstream from the inlet of the selected synthetic tube; 6. control unit for the flow probe; 7. BNC cable; 8. computer running LabView software; 9. secondary tube, 800 cm in length; 10. selected tube, 192 cm in length.

Reservoirs: In this experiment, two containers were used. One was positioned at the end of the subordinated tube to compensate for and contain the volume of water displaced during the forward (compression) and backward (retraction) strokes of the pump's piston. The other was placed directly downstream of the system pump and was used to include the main selected synthetic tube.

Water was selected as the working fluid due to its ease of use, replicability and compatibility with sensors. Whilst fluids with blood-mimicking viscosity could yield more physiologically relevant data, the primary requirement in the governing equations is the fluid's density. Water, with a density of 1000 kg/m^3, closely approximates that of blood, which is approximately 1060 kg/m^3.

A roughly half-sinusoidal pulse was generated in the forward direction using a syringe-based reciprocating pump, which was linked and driven by a Scotch yoke mechanism by means of an electric actuator (MAXON, DC-MAX, SWISS) powered a 12-volt alternating current supply. In all experiments, a single forward pulse was delivered at a frequency of 1.1 Hz. The injected water volume was approximately 40 cc over a duration of 0.9 s.

Pressure was measured using a transducer-tipped catheter (GAELTEC, SCOTLAND, UK), positioned 25 cm downstream from the inlet of the main tube. Flow velocity was recorded using ultrasound probes and a flowmeter control unit (TRANSONIC, HT323, NY, USA). Simultaneous measurements of pressure and flow were taken at the same location, 25 cm downstream of the tube inlet. To acquire the measured data, the LabView program was applied at a sampling rate of 500 Hz. These data were gained using the National Instruments (BNC-2090 DAQ, TEXAS, USA) system. Matlab software was used to write offline programs to analyse the measured data.

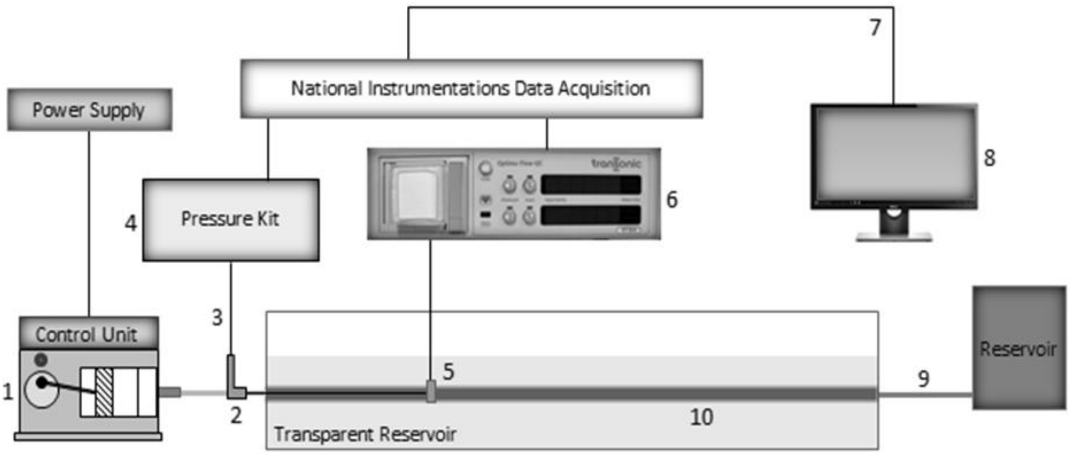

Fig. 1. Experimental setup schematic for estimating *c*, using the PU-loop technique, indicating all components. Main and secondary synthetic rubber tubes connected in line with the pump and cylindrical reservoir.

Catheter insertion can lead to localised pressure loss or flow disruption within the vessel, potentially compromising the fidelity of pressure waveforms and altering the physiological haemodynamic environment. Such effects must be carefully considered, particularly in in vitro experiments or in vivo applications where precise pressure waveforms are essential for interpretation.

To mitigate these issues, we minimised the insertion depth, maintained straight tubing alignment and calibrated the pressure sensor post-insertion to compensate for baseline offset.

Elastic Tubes: In this experiment, the main synthetic tube featured an isotropic, circular cross-sectional area along its 192 cm length. The tube wall was uniformly in 0.2 cm thick, with an inner diameter of 1.7 cm. A secondary uniform-lumen tube measured 400, 1 and 0.2 cm in length, diameter and wall thickness, respectively. Both tubes were composed of flexible rubber [Health Care, UK], selected based on availability, elastic behaviour and reproducibility of mechanical properties, criteria suitable for conducting repeatable pulse wave propagation experiments.

2.2.2 Tensile Testing Setup

Elastic rubber vessel flexibility was characterised through uniaxial tension testing, an appropriate method given the cylindrical structure and physiological loading conditions. Bending tests were deemed unnecessary because the vessel would not be subjected to flexural stresses under normal operating conditions.

Calculation of the modulus of elasticity enabled the application of the M-K equation to calculate *c*. Young's modulus (*E*) of the main tube was measured using tensile testing with an appropriate servo load cell (*Instron High Wycombe, UK)*. The relationship between applied load and corresponding extension was recorded using the Instron software *(Bluehill2)*, yielding an estimated *E* value of 3.3 MPa. The tested specimens had wall thickness, inner diameter and width of 0.2, 1.7 and 0.75 cm, respectively, as illustrated in Table 1. TMax., LMax., YTS and LY in Table 1 represent the tensile stress at the maximum thickness, maximum load, yield tensile stress and load at yield, respectively. The experiments comprised primarily three tests on the identical segments. However, in some instances, four tests were conducted, depending on the level of comfort with the gathered data. Prior to formal testing, specimens underwent a warm-up procedure involving repeated cycles of stretching and relaxation. This step was essential to eliminate any defects or manufacturing-induced tears that could compromise the accuracy of the measured modulus of elasticity.

Table 1,
Tensile test results for the tested elastic synthetic tube. MPa means 10^6 Pascals.

$T_{Max.}$ (MPa)	$L_{Max.}$ (N)	YTS (MPa)	LY (N)	Young's Modulus (MPa)
6.2±0.015	180±0.20	5.9±0.015	180±0.2	3.3±0.012

2.2.3 Compliance Testing Setup

In this work, the test was not used to validate the hypothesis that reduced arterial compliance contributes to significant atherosclerotic diseases, as emphasised by recent studies. Instead, it was employed to estimate the elastance of the selected synthetic flexible tube, enabling quantification of the magnitude of *c* that governs flow propagation through the tube.

The static pressure difference (*dP*) during compression and retraction procedures, along with the corresponding volume change (*dV*), were obtained using the setup shown in Fig. 2. Consequently, *c* will be calculated through the synthetic elastic tube using the Bramwell–Hill equation [27].

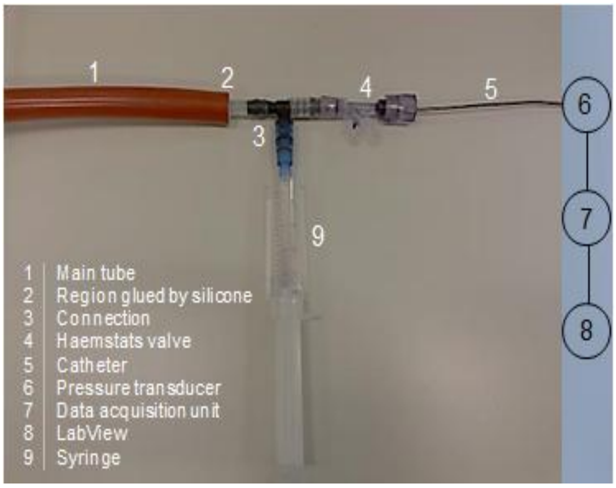

Fig. 2. Experimental setup applied, estimating compliance testing-based-pulse wave speed for the selected synthetic flexible tube, indicating all parts.

2.2.4 Instrumentation Calibration Procedures

Calibration procedures were conducted prior to each trial to ensure measurement reproducibility, accuracy and data reliability under strict experimental test conditions.

The catheter was positioned adjacent to a fixed column of water and used as a reference standard. Output voltage from the catheter was recorded at 10 cm incremental heights of the water column, corresponding to known pressures (1 cm H_2O = 98.1 Pa). A voltage–pressure calibration curve was constructed using linear regression, rendering the catheter response linear and drift-free. The calibration plot served as the basis for transforming catheter voltage output into precise pressure readings throughout the experimental tests.

The load cell was calibrated using a certified calibration weight under tension and compression modes. The test machine software (Instron Bluehill or equivalent) automatically generated a calibration curve by correlating measured force with known weights, enabling precise force measurements within the range specified by the load cell. Zero-load stability was also verified intermittently before and after the test.

Velocity sensors, used in the PU-loop setup, were calibrated using a pulsatile flow generator, providing repeatable and controlled velocity profiles. The output of the sensor was calibrated against a reference ultrasonic Doppler velocimeter or a known flow rate in a precision syringe pump system. The output voltage of the velocity sensor was referenced to actual velocity values (in m/s) to obtain the calibration function. Sensors were also positioned at the centreline of flow so that they could have maximum accuracy.

2.2.5 Standardisation and Adaptation of Testing

To ensure consistency, accuracy and replicability of the mechanical properties of the synthetic materials used in this comparative study, standardised testing procedures were implemented and selectively adjusted. Tensile tests on the elastomeric tubes were conducted with reference to ASTM D412, which outlines procedures for determining the tensile properties of vulcanised rubber and thermoplastic elastomers [31]. This standard provides recommendations for testing tensile strength, elongation and modulus as well as for specimen preparation and strain rate. Here, synthetic rubber tubes were tested on a universal testing machine with flat grips at 500 mm/min extension rate, following Method A of ASTM D412. However, due to the tubular form of the specimens, some modifications were made to accommodate circular cross-sections and prevent slippage or localised deformation during the tests. Special fixtures were employed to prevent stress concentrations at the grip areas and to achieve axial alignment.

Pressure–volume characterisation was carried out with reference to ISO 9276-1, providing general principles for describing the relationship between applied pressure and resulting volume changes for materials [32]. Although originally developed for particulate systems, the general approach of defining the pressure–volume relationship was adhered to characterise the elastic behaviour of the synthetic tubes under internal pressurisation. Incremental pressures were applied through a controlled pump system, and the ensuing volume displacement was quantified using calibrated syringes and high-resolution imaging to track radial deformation. The incompressibility of the tubes and their homogeneous wall structure enabled the faithful implementation of the modified protocol.

These adjustments allowed the use of widely acceptable standards and the alteration of the procedures to the geometry and the mechanical qualities of the synthetic models. Thus, the experimental results were not only robust but also directly translatable in the analytical models used in the study.

3. Results

According to the PU-loop technique shown in Fig. 3, the value of c equals (20±0.25 m/s). Data appearing in this figure represent the measurements collected 25 cm downstream of the main tube inlet. The linear portion in this loop indicates a period within the pulse cycle undisturbed by the presence of reflected waves. c can be calculated according to any two measurements of pressure and velocity in this linear portion, as demonstrated by the two red points.

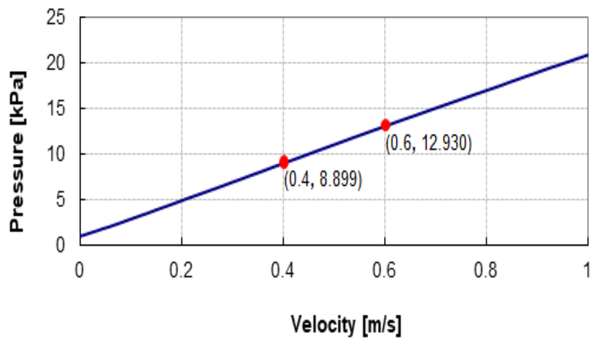

Fig. 3. PU-loop for measurements of *P* and *V* taken 25 cm downstream of the selected synthetic flexible tube inlet. The measurements displayed are limited to the segment where the effect of wave reflection is absent.

Table 1 presents the results of the tensile testing conducted on an isotropic rubber specimen with a thickness of 0.2 cm. The elasticity modulus for that tensile testing was 3.3 MPa. Theoretically, according to equation (2), if water with a density of 1000 kg/m^3 is forced through the main tube, the resulting pulse wave will travel at a speed of approximately 19.5 m/s within the lumen of the tube.

During compliance testing, the static pressure difference (*dP*) during the compression stroke was 101.5±0.40 kPa, and the corresponding volume change (*dV*) was 12 mL of water, from an initial volume (V_o) of 45 mL, as shown in Fig. 3. Accordingly, the wave pulse speed was 19.5±0.05 m/s using the Bramwell–Hill equation [27], assuming water with a density of 1000 kg/m^3 flowing through the main tube.

4. Discussion

The value of *c* obtained through experiments (in vitro) using the PU-loop technique was verified, considering the elasticity and compliance of the wall of the main tube. The main tube was tested, applying tensile and compliance tests.

Rubber materials form the uniform synthetic tube, developed using a circular cross-sectional area along its length. The lumen wall of the main tube was assumed to be isotropic and had a uniform elastic modulus.

The main tube was completely immersed in water of the transparent reservoir to increase the sensitivity and the response of the flow probe and eliminate the effects of the gravitational forces and the stresses that may be generated during the experiments as a result of its contact with the surface of the platform. This installation permitted the main tubes to expand and inflate in free mode. The effect of the hydrostatic pressure variations between the upper and lower surfaces of the main tube was neglected.

Table 1 illustrates a report on the modulus of elasticity value for the same test. The table clearly shows that the verification process involves using the experimental results of tensile testing to draw the relationship between the load applied and its corresponding extension. Elasticity of the elastic tube lumen was tested using tension load frame of (*Instron High Wycombe, UK*) the machine, considering *Bluehill2* software. This approach elaborates the report of calculating the value of (*E*) for the tested specimens and draw the relationship between the load applied and the extension according to that load.

Estimating the modulus of elasticity enables calculating the value of *c* through the lumen of the rubber tube using the Moens–Korteweg equation. This equation expresses the relationship between the arterial wall distensibility and the wave pulse speed using its elastic modulus.

Moreover, the compliance of the main tube was tested under static pressure to verify the magnitude of the traveling wave pulse speed through the main tube. The compliance or the buffering function of the artery's lumen is a critical physical parameter in the study of the cardiovascular system. This term denotes an increase in the volume of the artery's lumen accompanied by an increase in its pressure.

The compliance of the tube lumen is defined as the ratio of volume change to the change in applied pressure. Fig. 2 illustrates the setup for compliance testing. The setup consists of an elastic tube required to test its elasticity, which was initially filled with a volume of water and the catheter that measures the pressure inside the tube during this testing. The tip of the catheter was positioned in the centreline and midpoint of the tube to ensure an optimal and suitable location for collecting pressure readings. The setup included a medical syringe and a haemostat valve as well. The syringe was used to inject the water inside the compliant rubber tube with equal intervals as step input. The haemostat valve was used to adjust the position of the catheter's tip and to seal the setup to prevent leakage. The catheter functioned as a feedback or transducer element for this setting, ; it was connected to data acquisition through the pressure control unit by BNC cable, gained data transferred into LabView as a volt signal and monitored through the computer screen.

The results were almost identical in the case of compression and retraction procedures, as shown in Fig. 4. In the figure, the magnitude of *c* is equal to 19.5±0.05 m/s at the compression and retraction courses of the main tube to its initial volume. Data are presented as the mean of three measurements, and the dashed line indicates the linear regression of data, described by the equation and correlation coefficient, $R^2 = 0.9922$ for compression procedure and $R^2 = 0.9883$ for retraction procedure. Consequently, the two magnitudes of *c* in the compression and retraction procedures for the main tube are relatively identical. The procedure for the compression and retraction phases was designed to closely mimic physiological conditions. This complementary behaviour reinforced the results of the current testing.

5. Limitations

This study's findings may be limited by the sample size or the specific characteristics of the tested arterial specimens or materials. Variability in vessel geometry, composition and disease states may affect the generalisability of the results to broader populations or different anatomical sites.

The experimental conditions for the PU-loop and mechanical testing methods may not fully emulate physiological in vivo conditions. For example, pre-stress, residual strains and viscoelastic characteristics of the arterial wall are crucial phenomena to be simulated in vitro because of their influence on *c* estimations.

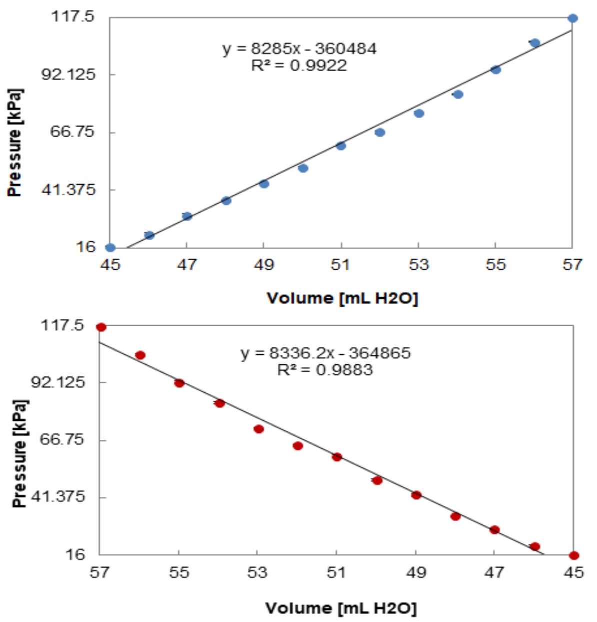

Fig. 4. Pressure–volume diagram for the selected synthetic elastic tube. *Upper* and *lower* panels represent compression and retraction procedure's data, respectively.

The PU-Loop method often relies on simplifying assumptions—such as neglecting wave reflections, assuming a uniform cross-sectional geometry or ignoring longitudinal motion. These assumptions can introduce systematic errors when compared with tensile or compliance-based mechanical tests.

Measurement noise, calibration errors and/or operator variability contribute to the PU-loop and mechanical testing methods. In the PU-Loop approach, noise in the pressure or velocity signals can significantly affect the accuracy of *c* estimation. On the contrary, mechanical testing is susceptible to non-linearities, hysteresis and slippage during tensile loading.

No universally accepted gold standard is available for measuring *c* in experimental setups. Thus, direct comparisons between methods become difficult, given that each technique might inherently emphasise different biomechanical properties (e.g., dynamic vs. static stiffness).

Biological tissues such as arteries exhibit anisotropic and heterogeneous properties that may not be fully captured by either method. Whilst tensile testing can better characterise anisotropy through different loading directions, PU-loop estimates may oversimplify these features by focusing on a single dynamic wave speed parameter.

Arteries often require preconditioning to reach a stable mechanical response. Differences in preconditioning protocols, or the absence of such procedures, can influence compliance and tensile measurements, thereby affecting comparative results between PU-Loop and mechanical approaches.

PU-loop tests are inherently dynamic, reflecting wave propagation characteristics, whereas tensile and compliance tests typically determine quasi-static mechanical properties. This fundamental difference complicates direct comparisons and interpretations of mechanical behaviour complicated.

Both approaches may rely on specific models (e.g., Moens–Korteweg equation) or assumptions that might not fully account for the complexities of real arterial behaviour, especially in diseased or remodelled vessels.

Variations in the experience of the operators or interpretation of the data may cause bias in the comparison; for example, determining the foot of the wave in PU-Loop testing or the linear part of the stress–strain curve in tensile testing.

The flexible tubes used in this experiment are stiffer than in vivo lumens. Nevertheless, the main objective was to validate the use of the PU-loop method in calculating *c* that propagates in flexible tubes, considering tensile and compliance testing. Despite these limitations, our study demonstrated excellent consistency in the outcomes of all techniques, supporting the ingenuity of the PU-loop method.

Finally, potential long-term effects of fatigue under cyclic pulsatile loading were not considered because the tests were conducted over short durations. Evidently, long-term cyclic loading would affect the results. The problem and objective statements of our future article will be directed towards investigating material fatigue and hysteresis under long-term cyclic loading to more closely simulate in vivo physiological conditions.

6. Conclusions

The *c* within the main tube, calculated using the PU-loop method based on simultaneous measurements of velocity and pressure technique, was 20±0.25 m/s. this value closely matched the estimates derived from established theoretical models: 19.5±0.012 m/s using the Moens–Korteweg equation and 19.5±0.05 m/s via the Bramwell–Hill equation. Furthermore, the results obtained from tensile testing and compliance measurements on the same synthetic vessel were in strong agreement with those from the PU-loop technique. These findings verify the use of the PU-loop method to calculate *c* in elastic synthetic vessels. The consistency of pulse wave velocity values across dynamic PU-loop and tensile and compliance approaches supports the PU-loop as a reliable, non-invasive alternative.

Finally, the comparative analysis presented here has revealed the effectiveness of the traditional (i.e., compliance and tension testing) and dynamic (PU-loop) techniques in modelling haemodynamic responses under controlled conditions. The results emphasise the relevance of accounting for pulse wave reflections and compliance impacts in the estimation of *c*, along with the associated numerical parameters. Whilst these findings provide valuable insights, further studies are guaranteed to validate these results under more physiologically representative and in vivo circumstances. In particular, the use of anatomically realistic models and blood-analogue fluids will be crucial for enhancing the translational relevance of the approach. These future investigations will help bridge the gap between clinical applications and experimental simulations.

References

[1] Laurent, S., Cockcroft, J., Van Bortel, L., Boutouyrie, P., Giannattasio, C., Hayoz, D., Pannier, B., Vlachopoulos, C., Wilkinson, I. and Struijker-Boudier, H., 2006. Expert consensus document on arterial stiffness: methodological issues and clinical applications. European Heart Journal, 27(21), pp.2588–2605. https://doi.org/10.1093/eurheartj/ehl254.

[2] Miyatani, M., Yasuda, T., Fukumura, K., Iida, H., Yamasoba, T., Sato, Y. and Ishii, N., 2009. Pulse Wave Velocity for Assessment of Arterial Stiffness. Journal of Clinical Hypertension, 11(7), pp.411–417. https://doi.org/10.1111/j.1751-7176.2009.00139.x.

[3] Kim, H.L. and Kim, S.H., 2019. Pulse Wave Velocity in Atherosclerosis. Frontiers in Cardiovascular Medicine, 6, p.41. https://doi.org/10.3389/fcvm.2019.00041.

[4] Negoita, M., Hughes, A.D., Parker, K.H. and Khir, A.W., 2018. A method for determining local pulse wave velocity in human ascending aorta from sequential ultrasound measurements of diameter and velocity. Physiological Measurement, 39(11), p.114009. https://doi.org/10.1088/1361-6579/aae8a0.

[5] Manoj, R., Raj, K.V., Nabeel, P.M., Thomas, A., Karthikeyan, P., Suresh, S., Joseph, J. and Jayaraj, J., 2025. Measurement of pressure dependent variations in local pulse wave velocity within a cardiac cycle from forward travelling pulse waves. Scientific Reports, 15, p.3066. https://doi.org/10.1038/s41598-025-87143-z.

[6] Janjua, G.M.W., McLaughlin, J., Finlay, D.D., Guldenring, D. and Hadia, R., 2017. Novel non-invasive Pressure-Volume Loop measurement for local Pulse Wave Velocity estimation. 44th Computing in Cardiology Conference (CinC 2017), Rennes, France. https://doi.org/10.22489/CinC.2017.217-385.

[7] Segers, P., Swillens, A., Taelman, L. and Vierendeels, J., 2014. Wave reflection leads to over- and underestimation of local wave speed by the PU- and QA-loop methods: theoretical basis and solution to the problem. American Journal of Physiology-Heart and Circulatory Physiology, 306(3), pp.H426–H433. https://doi.org/10.1152/ajpheart.00751.2013.

[8] Van Den Bos, G.C., Wesseling, K.H., De Wit, B. and Settels, J.J., 2003. Automating the determination of wave speed using the PU-loop method. Proceedings of the 25th Annual

International Conference of the IEEE Engineering in Medicine and Biology Society, 4, pp.3700–3703.

[9] Arias, D.C., Vignon-Clementel, I.E., Figueroa, C.A., Taylor, C.A. and Jansen, K.E., 2019. A 1D arterial network model analysis. Journal of Biomechanics, 83, pp.1–8. https://doi.org/10.1016/j.jbiomech.2019.01.002.

[10] Aguado-Sierra, J., Alastruey, J., Davies, J., Nordsletten, D., Brown, M., Parker, K.H. and Figueroa, C.A., 2006. Arterial pulse wave velocity in coronary arteries. IEEE Transactions on Medical Imaging, 25(10), pp.1284–1293. https://doi.org/10.1109/TMI.2006.881311.

[11] Ma, Y., Li, Y., Wang, Y., Wang, Y., Wang, Y. and Wang, Y., 2018. Relation between blood pressure and pulse wave velocity in the general population. Proceedings of the National Academy of Sciences, 115(52), pp.13289–13294. https://doi.org/10.1073/pnas.1814392115.

[12] Tripathi, A., Khir, A.W. and Parker, K.H., 2017. A Pulse Wave Velocity Based Method to Assess the Mean Arterial Pressure. Frontiers in Physiology, 8, p.855. https://doi.org/10.3389/fphys.2017.00855.

[13] Spronck, B., Heusinkveld, M.H.A., Hughes, A.D., Heethaar, R.M. and Westerhof, B.E., 2023. 2024 Recommendations for Validation of Noninvasive Arterial Stiffness Measurement Devices. Journal of Hypertension, 41(1), pp.1–10. https://doi.org/10.1097/HJH.0000000000003271.

[14] Wilkinson, I.B., McEniery, C.M., Schillaci, G., Boutouyrie, P., Segers, P., Donald, A., Chowienczyk, P., Parker, K.H., Laurent, S. and Cockcroft, J.R., 2020. Uses of Arterial Stiffness in Clinical Practice. Arteriosclerosis, Thrombosis, and Vascular Biology, 40(3), pp.666–672. https://doi.org/10.1161/ATVBAHA.120.313130.

[15] Salvi, P., Grillo, A., Pini, A., Alonzo, A., Balbarini, A., Parati, G. and Mancia, G., 2022. Non-Invasive Assessment of Arterial Stiffness: Pulse Wave Velocity. Journal of Clinical Medicine, 11(8), p.2225. https://doi.org/10.3390/jcm11082225.

[16] Cho, J., Lee, J., Park, K. and Kim, S., 2020. A comparative study of brachial–ankle pulse wave velocity. MDPI Sensors, 20(7), 2073.

[17] Karaki, M., Watanabe, T., Yoshida, K., Ito, S. and Takahashi, H., 2025. The validity of carotid-femoral pulse wave velocity in the assessment of arterial stiffness. Journal of Applied Physiology, 128(1), pp.73–80. https://doi.org/10.1152/japplphysiol.00073.2024.

[18] Mourad, J.J., Blacher, J., Blin, P., Hoeks, A. and Safar, M.E., 2001. Creatinine clearance, pulse wave velocity, carotid compliance and essential hypertension. Kidney International, 59(5), pp.1834–1841. https://doi.org/10.1046/j.1523-1755.2001.0590051834.x.

[19] Zhou, Y., Wang, Y., Zhang, L., Li, X., Zhang, Y. and Wang, Y., 2020. P125 Local Pulse Wave Velocity in the Arterial Tree. Atlantis Press.

[20] Vappou, J., Luo, J. and Konofagou, E.E., 2010. Pulse Wave Imaging for Noninvasive and Quantitative Measurement of Arterial Stiffness in vivo. American Journal of Hypertension, 23(4), pp.393–398. https://doi.org/10.1038/ajh.2010.8.

[21] Aimagambetova, B., Ilyasova, N., Kadyrova, I., Khamzina, Y., Kadyrov, A., Khamzina, Y., Kadyrov, A. and Khamzina, Y., 2024. Arterial stiffness measured by pulse wave velocity correlated with cognitive function in elderly patients. BMC Neurology, 24, p.390. https://doi.org/10.1186/s12883-024-03905-8.

[22] Gheysen, L., De Backer, J., De Wilde, D., De Backer, J. and De Wilde, D., 2023. Pulse wave velocity: A clinical measure to aid material characterization of vascular tissues. Journal of the Mechanical Behavior of Biomedical Materials, 137, p.105519. https://doi.org/10.1016/j.jmbbm.2022.105519.

[23] Roberts, P.A., Davies, J.E., Hughes, A.D., Parker, K.H. and Francis, D.P., 2015. Real-time aortic pulse wave velocity measurement during exercise stress testing. Journal of Biomechanics, 48(5), pp.847–853. https://doi.org/10.1016/j.jbiomech.2015.01.013.

[24] Bogatu, L.I., Ding, Z., Li, Y., Wang, Y. and Duan, Y., 2020. A modelling framework for assessment of arterial stiffness using pulse wave velocity. Computer Methods and Programs in Biomedicine, 190, p.105362. https://doi.org/10.1016/j.cmpb.2020.105362.

[25] Woodman, R.J., Kingwell, B.A., Beilin, L.J., Hamilton, S.E., Dart, A.M. and Watts, G.F., 2005. Assessment of central and peripheral arterial stiffness. American Journal of Hypertension, 18(2), pp.249–254. https://doi.org/10.1016/j.amjhyper.2004.07.023.

[26] Salvi, P., Magnani, E., Valbusa, F., Agnoletti, D., Alecu, C. and Benetos, A., 2008. Comparative study of methodologies for pulse wave velocity. PubMed, 18528411.

[27] Bramwell, J.C. and Hill, A.V., 1922. The velocity of the pulse wave in man. Proceedings of the Royal Society of London. Series B, Containing Papers of a Biological Character, 93(652), pp.298–306. https://doi.org/10.1098/rspb.1922.0022.

[28] Korteweg, D.J., 1878. Ueber die Fortpflanzungsgeschwindigkeit des Schalles in elastischen Röhren. Annalen der Physik und Chemie, 241(12), pp.525–542.

[29] Khir, A.W., O'Brien, A., Gibbs, J.S.R. and Parker, K.H., 2001. Determination of wave speed and separation of waves in arteries. Journal of Biomechanics, 34(9), pp.1145–1155. https://doi.org/10.1016/S0021-9290(01)00076-8.

[30] Hacham, W. S., Abdulla, N. N., Al-Ammri, A. S., and Khir, A. W., 2015. Wave speed and reflections proximal to aneurism and stenosis of flexible tubes, Proceedings of the 37th Annual International Conference of the IEEE Engineering in Medicine and Biology Society (EMBC), 2015, Milan, Italy, pp.1009-1012, https://doi.org/10.1109/EMBC.2015.7318535.

[31] ASTM International, 2021. ASTM D412-16: Standard Test Methods for Vulcanized Rubber and Thermoplastic Elastomers—Tension, West Conshohocken, PA: ASTM International.

[32] International Organization for Standardization, 1998. ISO 9276-1: Representation of results of particle size analysis–Part1: Graphical representation, Geneva: ISO.

تقدير سرعة موجة النبضة: دراسة مقارنة لتقنية حلقة الضغط - سرعة مقابل اختبار الشد والامتثال على الأنابيب المرنة الاصطناعية

وسام سعدي خضير[1]*، فلاح الزويد[2]، وسام حامد الزبيدي[3]
[1] *قسم هندسة الميكاترونكس، كلية هندسة الخوارزمي، جامعة بغداد، بغداد، العراق*
[2] *مجموعة كلية ترافورد وستوكبورت، ستريتفورد، قسم البناء والاستدامة، مانشستر، المملكة المتحدة*
[3] *كلية ويغان ولي، المملكة المتحدة*
*البريد الالكتروني:wisam@kecbu.uobaghdad.edu.iq

المستخلص

سرعة موجة النبض (c) هي متغير مهم في مجال ديناميكا الدم ودراسة خصائص الجهاز القلبي الوعائي. وهي مرتبطة ارتباطًا مباشرًا بمرونة تجويف الشريان وعكسيًا بمرونة تجويف الشريان. حلقة PU للقياسات المتزامنة للسرعة (U) والضغط (P) المستخدمة لحسابها. تستفيد هذه التقنية من الخطية بين U وP خلال الفترة المبكرة من انقباض القلب، حيث لا توجد موجة خلفية منعكسة بسبب تشعبات الشرايين و/أو انسدادها. تم اختبار صحة طريقة حلقة PU باستخدام اختبار الشد والمطاوعة. تم إجراء اختبار الشد باستخدام خلية تحميل، مع تقدير معامل مرونة يونغ (E) للأنبوب المرن. يستخدم الأخير لحساب c وفقًا لمعادلة موينز-كورتويج. أثناء النبض - لتقدير العلاقة بين P والحجم (V) - أجرينا اختبار الامتثال تحت الضغط الساكن. تنبأت هذه العلاقة بدورات الضغط والانكماش للتحقق من صحة الاختبار، الذي طُبّق على تجويف الأنبوب المرن. وبالتالي، لحساب قابلية تمدد تجويف الأنبوب المرن، استُخدم التغير في حجم التجويف الداخلي الناتج عن التغير في P، ومن ثمّ فإن c يتوافق مع معادلة براموبل-هيل. على الرغم من القيود، مثل: حجم عينة العينات المختبرة؛ الظروف التجريبية غير فسيولوجية تمامًا؛ حساسية الاختبارات بسبب ضوضاء القياس؛ إهمال تباين الخواص وعدم تجانس الأوعية الدموية؛ عدم مراعاة التعقيدات الكاملة لسلوك الشرايين الحقيقي؛ واستخدام أنابيب مرنة اصطناعية أكثر صلابة من التجاويف داخل الجسم الحي، فإن قيمة c المحسوبة (c المحسوبة)، باستخدام تقنية حلقة PU، كانت متوافقة مع القيم المكتسبة من الحسابات القائمة على اختبارات الامتثال والشد. وفقًا لاختبارات الامتثال والشد، بلغت السرعة ١٩,٥±٠,٠٥ متر/ثانية و١٩,٥±٠,٠١٢,١ متر/ثانية على التوالي، ووفقًا لتقنية حلقة PU، بلغت السرعة ٢٠±٠,٢٥ متر/ثانية. ونتيجةً لذلك، تم التحقق من صحة منهجية حلقة PU في تقييم c